

Geophysical Research Letters



RESEARCH LETTER

10.1029/2019GL086685

Key Points:

- Electroactive humic substances contribute significantly to iron-binding ligands released during microbial decomposition of mesopelagic particles
- Microbial degradation of settling biogenic particles supplies more electroactive humic substances than those where the lithogenic fraction is predominant
- Concurrent release of ligands and consumption by microbes can, in some cases, decrease the concentration of electroactive humic ligands

Supporting Information:

- Supporting Information S1

Correspondence to:

H. Whitby,
hannah.whitby@liverpool.ac.uk

Citation:

Whitby, H., Bressac, M., Sarthou, G., Ellwood, M. J., Guieu, C., & Boyd, P. W. (2020). Contribution of electroactive humic substances to the iron-binding ligands released during microbial remineralization of sinking particles. *Geophysical Research Letters*, 47, e2019GL086685. <https://doi.org/10.1029/2019GL086685>

Received 19 DEC 2019

Accepted 23 MAR 2020

Accepted article online 28 MAR 2020

Contribution of Electroactive Humic Substances to the Iron-Binding Ligands Released During Microbial Remineralization of Sinking Particles

Hannah Whitby^{1,2} , Matthieu Bressac^{3,4} , Géraldine Sarthou² , Michael J. Ellwood⁵ , Cécile Guieu^{4,6} , and Philip W. Boyd^{3,7} 

¹Department of Earth, Ocean and Ecological Sciences, School of Environmental Sciences, University of Liverpool, Liverpool, UK, ²CNRS, Univ Brest, IRD, Ifremer, LEMAR, Plouzané, France, ³Institute for Marine and Antarctic Studies, University of Tasmania, Hobart, Tasmania, Australia, ⁴Sorbonne Université, CNRS, Laboratoire d'Océanographie de Villefranche, LOV, Villefranche-sur-mer, France, ⁵Research School of Earth Sciences, Australian National University, Canberra, ACT, Australia, ⁶The Center for Prototype Climate Modeling, New York University in Abu Dhabi, Abu Dhabi, UAE, ⁷Antarctic Climate and Ecosystems Collaborative Research Center, University of Tasmania, Hobart, Tasmania, Australia

Abstract Iron is a key micronutrient in seawater, but concentrations would be negligible without the presence of organic ligands. The processes influencing the ligand pool composition are poorly constrained, limiting our understanding of the controls on dissolved iron distributions. To address this, the release of iron and iron-binding ligands during the microbial remineralization of sinking particles was investigated by deploying *in situ* particle interceptor/incubator devices at subsurface sites in the Mediterranean Sea and Subantarctic. Analyses revealed that the pool of released ligands was largely dominated by electroactive humic substances ($74 \pm 28\%$). The release of ligands during remineralization ensured that concurrently released iron remained in solution, which is crucial for iron regeneration. This study presents compelling evidence of the key role of humic ligands in the subsurface replenishment of dissolved iron and thus on the wider oceanic dissolved iron inventory, which ultimately controls the magnitude of iron resupplied to the euphotic zone.

Plain Language Summary Microscopic plants and animals in seawater require nutrients to survive. One of these key nutrients is iron, dissolved in seawater at very low concentrations. The growth of around half of the microscopic life in the upper ocean is dependent on the availability of this dissolved iron. These organisms form the bottom of the food chain, and their growth is linked to marine productivity and the drawdown of carbon into the deep ocean, in turn influencing climate change. Because iron tends to not dissolve easily in seawater, it must bind with compounds known as ligands, which help keep iron dissolved. However, processes controlling the composition of this ligand pool are poorly understood. As material sinks through the water column, it is broken down by marine microbes, releasing iron and ligands. Here we have studied the release of iron, ligands, and a specific type of ligand known as humic substances, during the microbial degradation of sinking particles. By doing this, we have identified a large fraction of the released ligand pool. This furthers our understanding of the processes controlling dissolved iron concentrations and distributions in ocean waters, providing key information for biogeochemical modeling and for calculating carbon sequestration in seawater.

1. Introduction

Dissolved iron (DFe) biogeochemistry controls around half of ocean primary productivity (Moore et al., 2013). In seawater, DFe is predominantly associated with a heterogeneous pool of organic ligands (Rue & Bruland, 1995; van den Berg, 1995; Wu & Luther, 1995). The ligand pool keeps Fe dissolved at concentrations that are much higher than its low solubility should allow (Millero, 1998), while the strength and type of Fe-ligand complexes influence Fe bioavailability to marine microorganisms (Hutchins et al., 1999). Determining the chemical nature of these unknown organic ligands is important for understanding the mechanisms behind Fe-acquisition by microorganisms (Granger & Price, 1999; Maldonado & Price, 1999).

©2020. The Authors.

This is an open access article under the terms of the Creative Commons Attribution License, which permits use, distribution and reproduction in any medium, provided the original work is properly cited.

On a global scale, identifying the sources and sinks of the key components of the Fe-binding ligand pool is essential to understand the processes controlling global DFe distributions in the ocean (Gledhill & Buck, 2012; Hassler et al., 2017).

The organic ligand pool responsible for Fe complexation is commonly measured using indirect electrochemical methods, which classify ligands based on their concentration and binding strength (Gledhill & Buck, 2012). It is recognized that L_1 ($\log K_{Fe^L} > 12$) represents the strongest class, L_2 ($\log K_{Fe^L}$ 11–12) an intermediate-strength class, followed by L_3 ($\log K_{Fe^L} < 11$) for the weaker Fe-binding classes (Gledhill & Buck, 2012). Although most Fe-binding compounds in seawater are included within the key categories of siderophores, exopolymeric substances (EPS), and humic substances, these groups can overlap (Gledhill & Buck, 2012; Hassler et al., 2017). The processes controlling the production, degradation, and Fe-binding capacities for the different components of the ligand pool are still poorly defined. As a consequence, the sources and sinks of ligands in subsurface waters are not currently well represented in biogeochemical models, resulting in more uniform DFe distributions than observations indicate (Tagliabue et al., 2016).

Efforts are now underway to tease apart the production and fate of the key groups of ligands that form the bulk ligand pool. Microbial remineralization of sinking particles represents a mechanism for supplying significant stocks of DFe to the water column (Boyd et al., 2017), increasing the intermediate and deep ocean Fe inventories, which can be resupplied to the surface ocean by upwelling and vertical mixing (Tagliabue et al., 2014). Microbial remineralization of organic matter also supplies ligands, which form complexes with this newly replenished DFe, keeping it in solution (Bressac et al., 2019). These ligands are predominantly intermediate-strength L_2 ligands (Boyd et al., 2010) but can include strong Fe-binding siderophores (Bundy et al., 2018; Velasquez et al., 2016). While the production of strong Fe-binding ligands during remineralization provides an important mechanism for stabilizing subsurface DFe stocks, the low concentrations of siderophores detected in seawater so far suggest that they may only play a minor role in the complexation of the DFe pool (Boiteau et al., 2019; Mawji et al., 2008).

Evidence points to humic substances as a major contributor to Fe complexation in seawater (Kitayama et al., 2009; Laglera & van den Berg, 2009; Nakayama et al., 2011; Slagter et al., 2019; Sukekava et al., 2018). Around 30–50% of dissolved organic carbon in seawater is composed of humic-like material (Zigah et al., 2017). However, humic substances are operationally defined, with numerous methods commonly used for their quantification. While this has limitations from a geochemistry perspective, valuable information can still be gleaned by each method. Here, electrochemical techniques were used to measure the electroactive humic substances (eHS), assumed to represent the metal-binding fraction of humics, which compose around 5% of dissolved organic carbon in seawater (Dulaquais et al., 2018; Laglera & van den Berg, 2009). The important role of eHS for Fe complexation in terrestrially influenced marine regions is well established (Abualhaija et al., 2015; Batchelli et al., 2010; Bundy et al., 2015; Dulaquais et al., 2018; Hassellöv, 2010; Laglera & van den Berg, 2009). However, in isolated environments such as the Southern Ocean where DFe is a limited resource, almost all humic material is derived from the recent microbial degradation (i.e. remineralization) of sinking autochthonous organic matter (Nelson et al., 2010). In contrast to terrestrial humics, which are largely derived from vascular plants and are highly aromatic (Bailey, 1996), marine humics are mostly derived from plankton and are carboxyl rich and aliphatic (Harvey et al., 1983; Hertkorn et al., 2006). Despite some key differences in composition, microbially produced precursors to humics in both systems (e.g., amino acids, lipids, and polysaccharides) also result in commonalities between marine and terrestrial humics (Hatcher et al., 1981). Such precursors (e.g., EPS) can themselves play a role in Fe cycling in the ocean (Hassler et al., 2011). Although marine eHS are likely to also be important for Fe complexation, little is known of the processes controlling the production and fate of the metal-binding fraction.

In a recent study, Bressac et al. (2019) compared concurrent DFe and Fe-binding ligand replenishment rates in the mesopelagic zone in the Southern Ocean and the Mediterranean Sea. These two contrasting biogeochemical provinces (Reygondeau et al., 2013) are characterized, in particular, by differing contributions from biogenic and lithogenic sinking material. In addition to water column samples, sinking particles were collected using a new *in situ* particle interceptor/incubator (trace metal (TM)-RESPIRE; Bressac et al., 2019) to investigate the drivers of DFe resupply within the upper mesopelagic zone. Here, we compare their

results to eHS measured within the same samples to elucidate the role of humic ligands in complexing DFe released during microbially mediated particle degradation. This study presents the first *in situ* measurements of eHS released during the bacterial degradation of sinking particles, revealing their potential contribution to the ligand pool in mesopelagic waters.

2. Methods

2.1. Water Column Sampling

All samples were obtained during GEOTRACES process studies, in the Subantarctic Zone southwest of Tasmania (EDDY and SAZ sites), aboard the *RV Investigator* (March 2016/2017; EDDY and SOTS projects) and in the central (Ionian Sea, ION site) and western (Algerian Basin, ALG site, and Thyrrenian Sea, TYR site) Mediterranean Sea, aboard the *RV Pourquoi Pas?* in May/June 2017 (PEACETIME project). Water column samples were collected using a Titanium Rosette mounted with Teflon-coated 12-L Niskin (EDDY/SAZ) or Go-Flo (ION/ALG/TYR) bottles that were deployed on a Kevlar cable. After recovery, Niskin/Go-Flo bottles were transferred inside a class 100 clean laboratory container. Seawater samples were directly filtered from the Niskins/Go-Flos through acid-cleaned 0.2- μ m capsule filters (Sartorius Sartobran-P-capsule 0.45/0.2 μ m) and stored in high-density polyethylene (HDPE) bottles at -20°C . Two sites were sampled in the high-nutrient low-chlorophyll waters of the Subantarctic Zone. The EDDY site (50.4°S , 147.1°E) was situated at the center of a cold-core cyclonic eddy characterized by very low productivity (Moreau et al., 2017) and extremely low surface DFe concentrations (<50 pM (Ellwood et al., 2020)). At the second site (SAZ and SAZ2; 46.1°S , 142.2°E), Fe limitation appears to also be the major control on productivity (Sedwick et al., 1999). At the SAZ sites, the sinking particulate Fe (PFe) flux is strongly dominated by biogenic PFe (Bressac et al., 2019). The Mediterranean Sea has a west-to-east gradient of increasing oligotrophy. During the stratification period, atmospheric deposition constitutes the main external source of new nutrients, resulting in strong DFe enrichment in the surface mixed layer (Bonnet & Guieu, 2006). In the Mediterranean, both the TYR (39.3°N , 12.6°E) and ION sites (35.5°N , 19.8°E) are characteristic of “no bloom areas,” with very low mean chlorophyll concentrations (D’Ortenzio & Ribera d’Alcalà, 2009), whereas the ALG site (37.9°N , 2.9°E) was slightly more productive. At the TYR site, only postincubation eHS and ligand data are available.

2.2. Sinking Particles

Sinking particles were collected using the particle interceptor/incubator RESPIRE along with a TM clean version (TM-RESPIRE) deployed on a surface-tethered free-drifting mooring between depths of 115–195 m (supporting information Table S1 and figure labels). The conceptual view and functioning of the RESPIRE and TM-RESPIRE are detailed in Boyd et al. (2015) and Bressac et al. (2019), respectively, and in supporting information Figure S1. Briefly, RESPIRE and TM-RESPIRE nonintrusively intercept settling particles and transfer them every 10 min via an indented rotating sphere (which excludes mesozooplankton) into an inner chamber of 1.6 L for 24–48 hr. Each device then incubates the collected particles for 24–48 hr at *in situ* pressure and temperature. Prior to deployment, seawater was collected with a TM-Rosette at the pre-selected depth of deployment and filtered through acid-cleaned 0.2- μ m capsule filters (Sartorius Sartobran-P-capsule 0.45/0.2 μ m) inside a class 100 clean container. Seawater was then gently transferred to the (TM-)RESPIRE using acid-cleaned tubing to minimize air bubbles within the incubation chamber. The water used to fill the (TM-)RESPIRE was denser than surface seawater, and the indented rotating sphere, which does not rotate during descent, is designed to prevent any exchange with surface waters as the (TM-)RESPIRE is deployed (Bressac et al., 2019).

Rates of remineralization by particle-attached bacteria are based on an oxygen consumption time series measured within the RESPIRE using an Aanderaa 3830 oxygen optode (Boyd et al., 2015) and are assumed to be equal in the TM-RESPIRE. Particulate organic carbon (POC) data were obtained from Bressac et al. (2019). The following equations were used to calculate the percentage of organic carbon consumption (% OC cons.):

$$\%OC \text{ cons.} = \left(\frac{POC \text{ respired}}{POC \text{ preincubation}} \right) \times 100 \quad (1)$$

$$POC \text{ respired} = O_2 \text{ cons.} \times 0.69 \quad (2)$$

$$POC \text{ preincubation} = POC \text{ postincubation} + O_2 \text{ cons.} \times 0.69 \quad (3)$$

Where $O_2 \text{ cons.} = O_2 \text{ pre-incubation} - O_2 \text{ post-incubation}$. Concentrations of $POC_{\text{post-incubation}}$ were measured, while $POC_{\text{pre-incubation}}$ concentrations were obtained using a C/ O_2 conversion factor of 0.69 (i.e., 117/170; (Anderson & Sarmiento, 1994)). See Bressac et al. (2019) for more details on the method and calculations. The percentage biogenic fraction was calculated using the ratio of organic/lithogenic material and assumes that all organic material is biogenic (supporting information Table S2).

Simultaneously, TM-RESPIRE provides DFe and Fe-binding ligand replenishment rates by comparing pre-incubation (i.e. *in situ*, supporting information Table S3) and postincubation concentrations. The initial eHS and ligand concentrations were sampled from the same seawater used to fill the (TM-)RESPIRE, except at SAZ2 and ION, where additional sampling with the TM-Rosette was performed alongside the deployed (TM-)RESPIRE. Subsamples for DFe and Fe-binding ligands were filtered through acid-cleaned 0.2- μm PC membranes (Nucleopore, Whatman). Fe-binding ligand samples were transferred to 500-mL HDPE bottles (cleaned according to the “GEOTRACES Cookbook”), double bagged, and stored at -20°C . Samples for eHS were subsampled from the ligand samples.

2.3. Analytical Methods

Measurements of the concentrations of DFe and Fe-binding ligands are described by Bressac et al. (2019). The concentrations of eHS were measured using cathodic stripping voltammetry of their complexes with copper (Whitby & van den Berg, 2015), which are directly comparable to Fe-eHS complexes but do not suffer interference from thiol groups. EPPS buffer (N-(2-hydroxyethyl)piperazine-N';-2-propanesulfonic acid in 1-M NH_4 ; 100 μL addition to 10-mL seawater buffered the pH to 8.15) and 30-nM added copper (spectrophotometry standard, pH 2) were added to 10-mL sample in a glass voltammetric cell. A μ -Autolab III potentiostat (Ecochemie, Netherlands) was connected to a 663 VA stand (Metrohm) with hanging mercury drop electrode. The reference electrode was Ag/AgCl with a 3-M KCl salt bridge and a glassy carbon counter electrode. Solutions were stirred with a rotating polytetrafluoroethylene rod. Following a 300-s nitrogen purge, the deposition potential was +0.05 V for 60 s, followed by a 1-s jump to -0.2 V and a 10-s equilibration time. A background subtraction (of a 1-s scan) was performed on all scans to improve the baseline. The concentration was determined by standard additions of the International Humic Substances Society Suwannee River humic acid (SRHA, II 2S101H) and fulvic acid (SRFA, II 2S101F) standards. The Fe equivalent for the eHS concentration was calculated from the reported binding capacity of SRFA, 14.6 nM iron per mg/L (Sukekava et al., 2018).

3. Results and Discussion

3.1. eHS Contribution to the Ambient Fe-Binding Ligand Pool

eHS composed a significant component of the total ligand pool (L_T) in the water column in both the Mediterranean, a basin surrounded by land, and the Southern Ocean, a region far from terrestrial influence. eHS concentrations contributed an average of $77 \pm 18\%$ of L_T across all water column samples (44% to 100%, Figures 1a and 2a). This range encompasses findings from previous studies in the Western Mediterranean, where eHS contributed 30–50% of L_T (Dulaquais et al., 2018), and in the Arctic, where eHS composed almost all of L_T (Slagter et al., 2017). Such a high contribution to L_T may be expected in regions encountering major terrestrial influences, but as the dissolved organic matter in the Southern Ocean is almost entirely marine derived (Nelson et al., 2010), the high eHS contribution to L_T suggests that marine-derived humics are also important players in Fe complexation. Across all water column samples, L_T had an average $\log K_{\text{FeL}}$ of 11.2 ± 0.2 , at the upper end of $\log K_{\text{FeL}}$ values reported for commercial humic isolates (reported \log

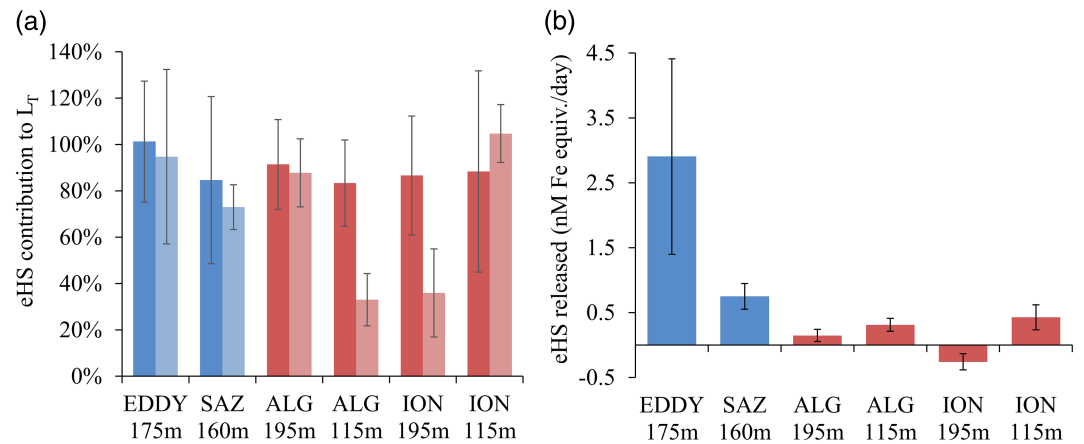


Figure 1. (a) The contribution of eHS to the total ligand pool in paired columns, with *in situ* (preincubation) values on the left and TM-RESPIRE postincubation on the right. (b) The concentration of eHS released per day of incubation. EDDY and SAZ sites are in the subpolar Southern Ocean, while ALG and ION are in the Mediterranean Sea. The TYR site is not included, as no *in situ* samples were obtained. The depth at which each trap was deployed is shown. The Fe-binding equivalent concentration for eHS is calculated using the conversion factor for Suwannee River Fulvic Acid (Sukekava et al., 2018).

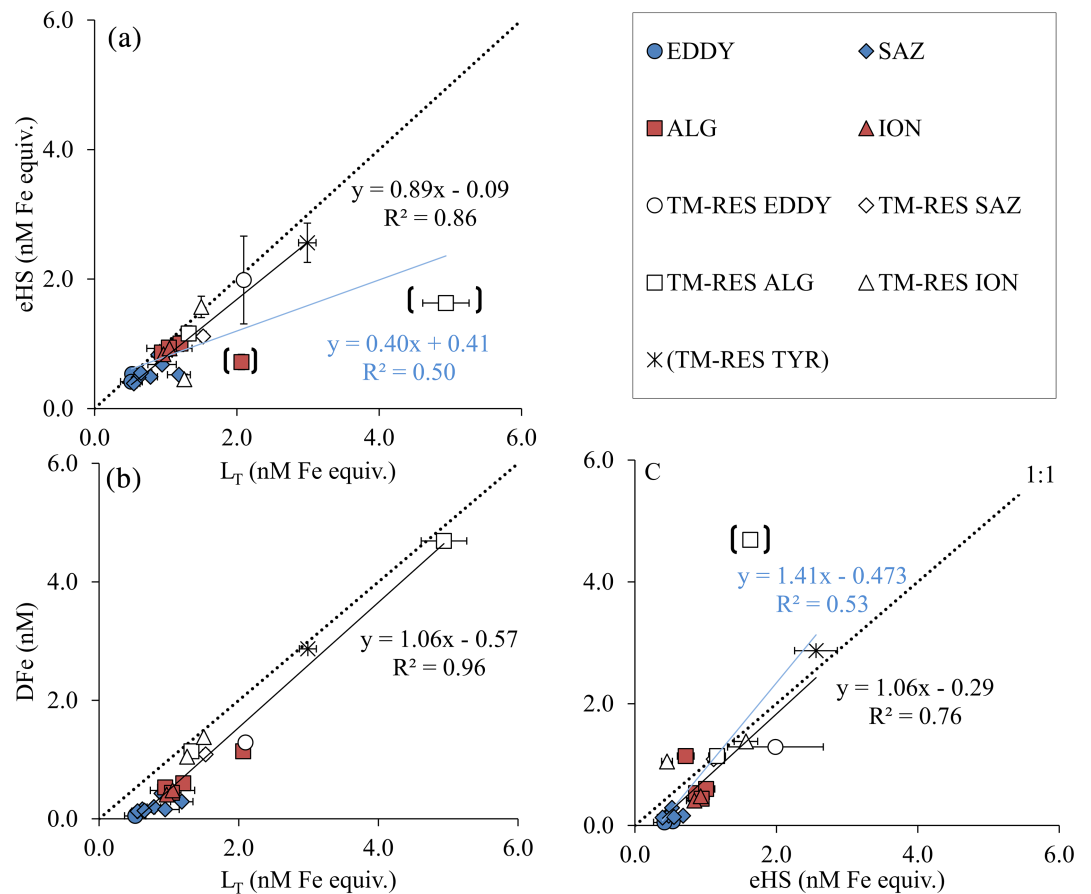


Figure 2. The relationship between the concentrations of (a) eHS and L_T , (b) DFe and L_T , and (c) DFe and eHS for both *in situ* (closed symbols) and postincubation (TM-RESPIRE, open symbols) samples in the Southern Ocean (circles = EDDY, diamonds = SAZ) and Mediterranean Sea (squares = ALG, triangles = ION, star = TYR). The black solid lines (representing best fits) do not include the outliers denoted by brackets, while blue lines include all data. Using all data ($n = 22$), (a) $p < 0.001$ while for (b) and (c) $p < 0.0001$. The dashed line represents the 1:1 relationship. No *in situ* samples were obtained at the TYR site. TM-RES stands for TM-RESPIRE.

K_{FeHS} of 10.6–11.1 (Laglera & van den Berg, 2009)) and consistent with eHS composing the bulk of the ligand pool. However, as L_T concentrations exceed both DFe and eHS concentrations indicating the presence of additional ligands, these findings do not reveal to what extent Fe complexation is reliant on eHS ligands specifically.

3.2. Microbial Particle Degradation: Release of Humic-like Ligands

A potentially important source of marine-derived humic ligands in seawater is microbial activity. The RESPIRE particle interceptor provides rates of microbial degradation of sinking particles based on an oxygen consumption time series.

We compared the difference in eHS concentrations postincubation to *in situ* (preincubation) samples taken from the water column immediately before or during deployment of the RESPIRE and TM-RESPIRE traps (eHS released, Figure 1b). eHS concentrations were significantly higher postincubation in five out of six of the particle traps.

In addition to a significant eHS component within the ambient L_T (Figures 1a and 2a), the release of eHS and other ligands during microbial degradation of particles will influence the eHS contribution to the ligand pool released concurrently with DFe. The concentration of L_T increased at all sites postincubation, with high correlation between DFe and L_T across all samples (Figure 2b). Postincubation, eHS also accounted for a significant fraction of L_T , contributing an average of $73 \pm 28\%$ (33% to 100%, Figures 1a and 2a) similar to contributions from *in situ* samples. eHS are thus a significant component of the Fe-binding ligands released during the microbial degradation of settling particles.

Log $K_{\text{Fe}^{\text{L}}}$ values were similar postincubation (mean 11.6 ± 0.2 compared to 11.2 ± 0.2 *in situ*, supporting information Table S3). Siderophore production has been detected during on-deck bacterial remineralization incubations, using particles collected with Lagrangian style net traps and *in situ* pumps (Bundy et al., 2018; Velasquez et al., 2016). The log $K_{\text{Fe}^{\text{L}}}$ values measured in our study are low for siderophore-like ligands; however, as log $K_{\text{Fe}^{\text{L}}}$ represents an average of the ligand pool when only a single ligand class is measured, low concentrations of siderophores could also have been released.

The concentration of ligands in excess of DFe (excess ligand, here referred to as L^*) is in theory available to complex fresh Fe inputs (Thuróczy et al., 2010). Assuming that all other ligands in these samples are stronger than eHS, the role of eHS in DFe complexation can be estimated by assuming that DFe first complexes all non-eHS ligands (Figure 3). Following this assumption, eHS would be responsible for an average of 68% of DFe complexation in postincubation samples, compared to 24% and 62% for Southern Ocean and Mediterranean ambient water column samples, respectively (although these contributions range from 0–100%, Figure 3). Thus, although DFe complexation could be accounted for by ligands other than eHS in some samples, in others, a significant fraction of DFe complexation is dependent on eHS.

Continuing with the assumption that DFe binds to all other ligands before eHS, between 0% and 51% of the eHS is saturated with DFe in the water column, suggesting that a large proportion of seawater eHS is free to buffer additional Fe inputs (Figure 3). However, the percentage saturation of eHS with DFe increases to 53–95% postincubation, as L_T becomes saturated with Fe (Figure 3). This demonstrates the importance of eHS in maintaining the DFe, supplied by microbial remineralization, in solution. These calculations do not take into account weaker ligands which eHS would outcompete but are consistent with studies that found that the eHS pool is not typically Fe saturated in upper waters (upper 400 m) (Boiteau et al., 2019; Sukekava et al., 2018).

In two of the six samples with *in situ* data, the eHS contribution to L_T decreased postincubation by around 40% (Mediterranean, Figure 1a). Although the eHS concentration increased postincubation in one of these samples (ALG 115 m), this increase was insufficient to account for the larger increases in DFe and L_T . In contrast, the second sample (ION 195 m) decreased in eHS concentration during the incubation. It is possible that some of the degraded eHS has a higher Fe-binding capacity than the lower value used here, underestimating the eHS contribution to L_T . Another explanation is a production of ligands other than eHS, such as siderophores (Bundy et al., 2018; Velasquez et al., 2016), EPS (Hassler, Alasonati, et al., 2011), nanoparticles, and other colloidal biopolymers (Hassellöv, 2010), the production of which could be linked to variation in source material or the bacterial community composition.

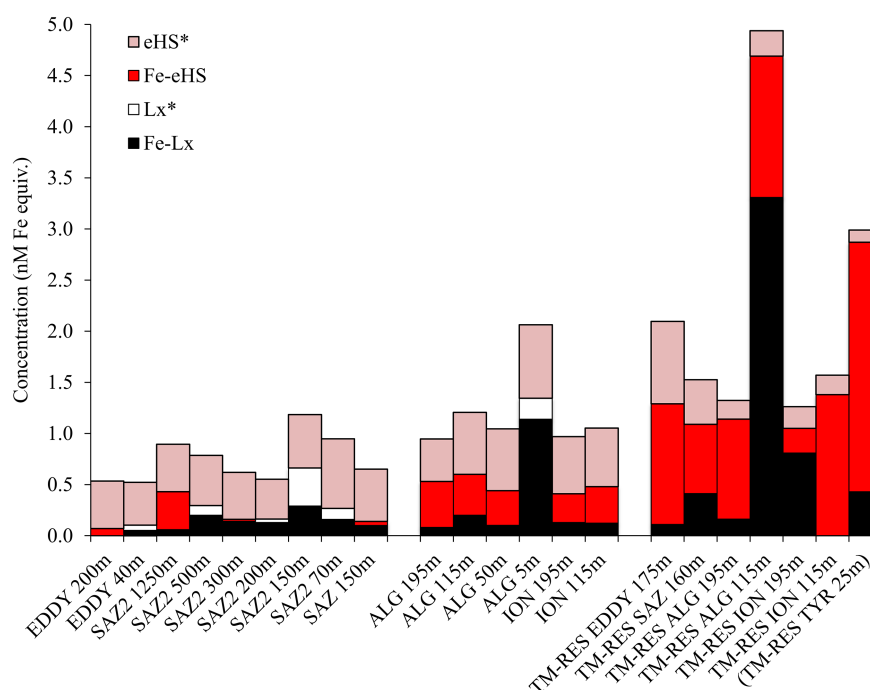


Figure 3. Bar chart of the calculated eHS contribution to Fe complexation, assuming all other ligands (L_x) are stronger than eHS and thus complexed first. Black bars (bottom, FeL_x) show the amount of Fe complexed by ligands other than eHS. White bars (L_x^*) show the amount of excess L_x remaining when DFe is fully complexed by L_x . Red bars show the Fe in Fe-HS complexes when L_x are saturated, while pink bars show excess eHS (eHS^*). Here, $L_x = L_T - eHS$, where L_T is from ligand titrations and is equivalent to the sum of $FeL_x + L_x^* + Fe-HS + eHS^*$. TM-RES stands for TM-RESPIRE, with the deployment depth included.

3.3. Relationship Between eHS and POC Degradation

Although we find that in the majority of samples microbial degradation of particles resulted in a release of eHS, the decreased eHS concentration in one sample suggests that microbial activity can also consume eHS. A negative relationship between eHS concentrations and the apparent oxygen utilization in a previous study in the Mediterranean suggested that bacterial degradation decreased eHS concentrations (Dulaquais et al., 2018). It was suggested this could be the result of the enhanced respiration rate of dissolved organic carbon in the Mediterranean (Dulaquais et al., 2018 and references therein). Fluorescence techniques have also found bacteria to both supply and consume material of humic-like fluorescence (Kinsey et al., 2018; Romera-Castillo et al., 2011; Rosenstock et al., 2005; Shimotori et al., 2009). Understanding the variability in the release and consumption of eHS by microbial activity could shed light on unidentified controls on the magnitude and composition of a key component of the Fe-binding ligand pool.

We compared the eHS released during remineralization as a percentage of total eHS postincubation to the percentage OC consumption (equations 1–3) and found a negative correlation (Figure 4a, $R^2 = 0.86$). Our results therefore suggest that microbial particle degradation results in a release of eHS, but at sites with high POC degradation, there is also concurrent eHS removal. Organic matter is selectively degraded by microorganisms (Harfmann et al., 2019; Kothawala et al., 2012) with nonhumic organic matter favored (Rosenstock et al., 2005); however, as the labile dissolved organic carbon pool decreases, some eHS becomes a viable source of carbon for microbes. This process is likely dependent on local physicochemical conditions and the availability of other carbon sources. Considering the important role of eHS in supporting DFe supplied by particle degradation, microbial removal of eHS ligands with increasing POC consumption could influence the amount of DFe resupplied by bacterial remineralization.

3.4. Lithogenic and Biogenic Ligand Sources

Mediterranean oligotrophic waters are subjected to intense Saharan dust deposition events (Guerzoni et al., 1999). As a consequence, lithogenic material represents a major constituent of the sinking flux in

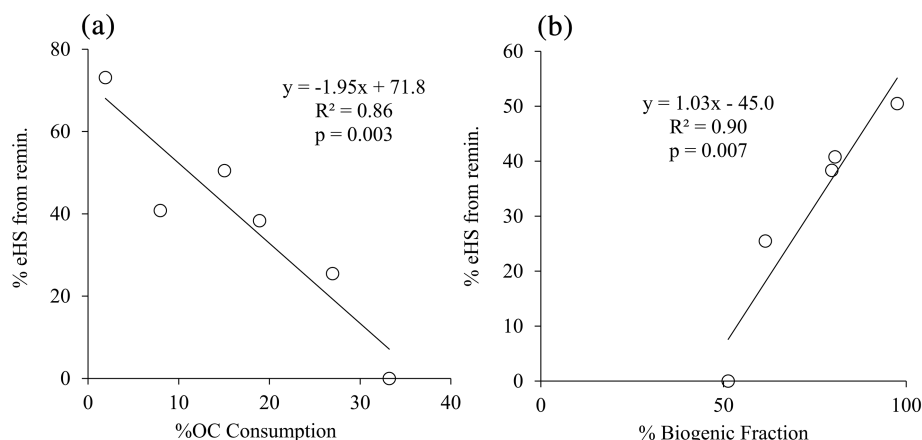


Figure 4. The percentage of postincubation eHS derived from the microbial remineralization of sinking particles (TM-RESPIRE) with respect to (a) the percentage organic carbon consumption for each of the TM-RESPIRE particle incubation traps and (b) the percentage biogenic fraction of the respective particles. The TYR site is not included in either figure, as no *in situ* values were available, and the EDDY site is not included in Figure 4b, as the biogenic fraction was not available. Negative values are shown as 0%.

the Mediterranean (Ternon et al., 2010). In the postincubation samples from the Mediterranean, L^* was negligible when considering the error of DFe and L_T concentrations. Near saturation of the ligand pool suggests that the supply of DFe from sinking particles could exceed the supply of ligands. Saturation of the ligand pool has been reported in the water column of the Mediterranean (Gerringa et al., 2017) and could partly explain the higher scavenging rates found in regions with a strong lithogenic particle loading (Wagener et al., 2010; Wuttig et al., 2013). Although the ligand pool maintains DFe at concentrations much higher than its low solubility should allow, its magnitude can also restrict the total amount of Fe that can be dissolved in a system.

In contrast, high-nutrient low-chlorophyll surface waters at the EDDY and SAZ sites are characterized by very low dust deposition and biologically limiting DFe levels (Bowie et al., 2009; Sedwick et al., 1999). The sinking flux in this region is largely dominated by biogenic material (Trull et al., 2001). When normalized to O_2 consumption or POC, Fe regeneration efficiencies were greater in the Southern Ocean than in the Mediterranean (Bressac et al., 2019). Similarly, both L^* and eHS release were also higher postincubation in the Southern Ocean than at sites in the Mediterranean (when normalized to O_2 consumption or POC, supporting information Tables S2 and S3). Figure 4b demonstrates that the degradation of biogenic material supplies more eHS than lithogenic material. The ligand and eHS data thus agree with the hypothesis that mesopelagic DFe replenishment is largely controlled by the ratio of biogenic:lithogenic contributions to particulate material (Boyd et al., 2010).

3.5. Method Limitations

L_T represents the minimum concentration of the ligand pool, as concentrations are dependent on the detection window and can be underestimated in the presence of eHS (Laglera et al., 2011). Using the lower Fe-binding capacity thought to be most representative of marine eHS (Sukekava et al., 2018) could underestimate the eHS contribution to L_T . In contrast, EPS purified from a bacterium isolated in the Southern Ocean contributed to the Fe-eHS peak when using the Fe-eHS voltammetric method (Hassler et al., 2011; Laglera et al., 2007), which could overestimate the contribution of HS to L_T . Labile EPS are building blocks in HS formation (Clark & Tan, 1969; Tan & Clark, 1969). As EPS are produced through all cellular life cycles (Myklestad, 1995) to protect microorganisms against heavy metals (Sheng et al., 2013) and increase Fe bioavailability (Hassler et al., 2015), this could be an important step in humic Fe-ligand production to investigate further.

4. Conclusions

We find that bacterial degradation of sinking particles supplies L_2 -type ligands and that a significant fraction of these ligands are eHS. The degradation of particles with a higher biogenic fraction resulted in a higher eHS

contribution to the overall ligand pool. Furthermore, eHS release correlated significantly with the %OC consumption. Our results suggest that microbial degradation results in a release of eHS, but at sites with high POC degradation, there is also concurrent eHS removal.

Our findings reveal that the saturation of eHS with DFe increases with increasing bacterial degradation, as the overall ligand pool nears Fe saturation. We find that while other ligands are supplied during bacterial degradation and also play a critical role in Fe complexation, eHS production can be crucial for complexing DFe released following particle degradation. The magnitude and composition of the ligand pool can thus restrict the total amount of Fe that can be dissolved in a system and demonstrate a need to integrate this process in biogeochemical models.

Author Contributions

H. W. performed the ligand and eHS measurements, analyzed the data, and wrote the manuscript. M. B. designed and carried out the study. C. G. and P. W. B. helped in the design of the study and co-led the cruises. M. J. E. helped in the different instrument deployments and sampling. G. S. worked on different versions of the manuscript. All authors commented on and contributed to the improvement of the manuscript.

Competing Interests

The authors declare that they have no competing interests.

Data Availability Statement

All data generated or analyzed during this study are included in this published article or in Bressac et al. (2019) (and their supporting information files).

Acknowledgments

We thank the captains and crew of the *RV Investigator* and *RV Pourquoi Pas?*, the CSIRO and DT INSU teams for the design and preparation of the mooring line, C. Young and P. Waller for building the TM-RESPIRE, and T. Wagener for helping with sampling. The authors wish to thank the CSIRO Marine National Facility (MNF) for its support in the form of sea time on *RV Investigator*, support personnel, scientific equipment, and data management. All data and samples acquired on the voyage are made publically available in accordance with MNF and AGU data policy. M. B. was funded by the European Union Seventh Framework Programme (FP7/2007-2013) under grant agreement no. (PIOF-GA-2012-626734). This study is a contribution to the PEACETIME project (<https://doi.org/10.17600/17000300>), a joint initiative of the MERMEX and ChArMEx components supported by CNRS-INSU, IFREMER, CEA, and Météo-France as part of the programme MISTRALS coordinated by INSU. H. W. was supported by the "Laboratoire d'Excellence" LabexMER (ANR-10-LABX-19) and by the EU FP7 Marie Curie actions (PCOFUND-GA-2013-609102), through the PRESTIGE programme coordinated by Campus France. This research was financially supported under Australian Research Council's Discovery (DP170102108 and DP130100679) and Laureate Awards (FL160100131).

References

- Abualhija, M. M., Whitby, H., & van den Berg, C. M. G. (2015). Competition between copper and iron for humic ligands in estuarine waters. *Marine Chemistry*, 172, 46–56.
- Anderson, L. A., & Sarmiento, J. L. (1994). Redfield ratios of remineralization determined by nutrient data analysis. *Global Biogeochemical Cycles*, 8(1), 65–80.
- Bailey, G. W. (1996). Life after death. *Lignin-humic relationships reexamined Critical Reviews in Environmental Science and Technology*, 26(2), 95–153.
- Batchelli, S., Muller, F. L. L., Chang, K.-C., & Lee, C.-L. (2010). Evidence for strong but dynamic iron–humic colloidal associations in humic-rich coastal waters. *Environmental Science & Technology*, 44(22), 8485–8490. <https://doi.org/10.1021/es101081c>
- Boiteau, R. M., Till, C. P., Coale, T. H., Fitzsimmons, J. N., Bruland, K. W., & Repeta, D. J. (2019). Patterns of iron and siderophore distributions across the California Current System. *Limnology and Oceanography*, 64(1), 376–389. <https://doi.org/10.1002/lno.11046>
- Bonnet, S., & Guieu, C. (2006). Atmospheric forcing on the annual iron cycle in the western Mediterranean Sea: A 1-year survey. *Journal of Geophysical Research*, 111, C09010. <https://doi.org/10.1029/2005JC003213>
- Bowie, A. R., Lannuzel, D., Remenyi, T. A., Wagener, T., Lam, P. J., Boyd, P. W., et al. (2009). Biogeochemical iron budgets of the Southern Ocean south of Australia: Decoupling of iron and nutrient cycles in the subantarctic zone by the summertime supply. *Global Biogeochemical Cycles*, 23, GB4034. <https://doi.org/10.1029/2009GB003500>
- Boyd, P. W., Ellwood, M. J., Tagliabue, A., & Twining, B. S. (2017). Biotic and abiotic retention, recycling and remineralization of metals in the ocean. *Nature Geoscience*, 10, 167.
- Boyd, P. W., Ibsanmi, E., Sander, S. G., Hunter, K. A., & Jackson, G. A. (2010). Remineralization of upper ocean particles: Implications for iron biogeochemistry. *Limnology and Oceanography*, 55(3), 1271–1288.
- Boyd, P. W., McDonnell, A., Valdez, J., LeFevre, D., & Gall, M. P. (2015). RESPIRE: An in situ particle interceptor to conduct particle remineralization and microbial dynamics studies in the oceans Twilight Zone. *Limnology and Oceanography: Methods*, 13(9), 494–508.
- Bressac, M., Guieu, C., Ellwood, M. J., Tagliabue, A., Wagener, T., Laurenceau-Cornec, E. C., et al. (2019). Resupply of mesopelagic dissolved iron controlled by particulate iron composition. *Nature Geoscience*, 12(12), 995–1000. <https://doi.org/10.1038/s41561-019-0476-6>
- Bundy, R. M., Abdulla, H. A. N., Hatcher, P. G., Biller, D. V., Buck, K. N., & Barbeau, K. A. (2015). Iron-binding ligands and humic substances in the San Francisco Bay estuary and estuarine-influenced shelf regions of coastal California. *Marine Chemistry*, 173, 183–194. <https://doi.org/10.1016/j.marchem.2014.11.005>
- Bundy, R. M., Boiteau, R. M., McLean, C., Turk-Kubo, K. A., McIlvin, M. R., Saito, M. A., et al. (2018). Distinct siderophores contribute to iron cycling in the mesopelagic at station ALOHA. *Frontiers in Marine Science*, 5(61). <https://doi.org/10.3389/fmars.2018.00061>
- Clark, F. E., & Tan, K. H. (1969). Identification of a polysaccharide ester linkage in humic acid. *Soil Biology and Biochemistry*, 1(1), 75–81.
- D'Ortenzio, F., & Ribera d'Alcalá, M. (2009). On the trophic regimes of the Mediterranean Sea: A satellite analysis. *Biogeosciences*, 6(2), 139–148.
- Dulaquais, G., Waeles, M., Gerringa, L. J. A., Middag, R., Rijkenberg, M. J. A., & Riso, R. (2018). The biogeochemistry of electroactive humic substances and its connection to iron chemistry in the North East Atlantic and the Western Mediterranean Sea. *Journal of Geophysical Research: Oceans*, 123, 5481–5499. <https://doi.org/10.1029/2018JC014211>
- Ellwood, M. J., Strzpek, R. F., Strutton, P. G., Trull, T. W., Fourquez, M., & Boyd, P. W. (2020). Distinct iron cycling in a Southern Ocean eddy. *Nature Communications*, 11(1), 825. <https://doi.org/10.1038/s41467-020-14464-0>
- Gerringa, L. J. A., Slagter, H. A., Bown, J., van Haren, H., Laan, P., de Baar, H. J. W., & Rijkenberg, M. J. A. (2017). Dissolved Fe and Fe-binding organic ligands in the Mediterranean Sea–GEOTRACES G04. *Marine Chemistry*, 194, 100–113. <https://doi.org/10.1016/j.marchem.2017.05.012>

- Gledhill, M., & Buck, K. N. (2012). The organic complexation of iron in the marine environment: A review. *Frontiers in Microbiology*, 3, Granger, J., & Price, N. M. (1999). The importance of siderophores in iron nutrition of heterotrophic marine bacteria. *Limnology and Oceanography*, 44(3), 541–555.
- Guerzoni, S., Chester, R., Dulac, F., Herut, B., Loÿe-Pilot, M. D., Measures, C., et al. (1999). The role of atmospheric deposition in the biogeochemistry of the Mediterranean Sea. *Progress in Oceanography*, 44(1–3), 147–190. [https://doi.org/10.1016/S0079-6611\(99\)00024-5](https://doi.org/10.1016/S0079-6611(99)00024-5)
- Harfmann, J., Kurobe, T., Bergamaschi, B., Teh, S., & Hernes, P. (2019). Plant detritus is selectively consumed by estuarine copepods and can augment their survival. *Scientific Reports*, 9(1), 9076. <https://doi.org/10.1038/s41598-019-45503-6>
- Harvey, G. R., Boran, D. A., Chesal, L. A., & Tokar, J. M. (1983). The structure of marine fulvic and humic acids. *Marine Chemistry*, 12(2), 119–132.
- Hassler, C., van den Berg, C. M. G., & Boyd, P. W. (2017). Toward a regional classification to provide a more inclusive examination of the ocean biogeochemistry of iron-binding ligands. *Frontiers in Marine Science*, 4, 60–19.
- Hassler, C. S., Alasonati, E., Nichols, C. A. M., & Slaveykova, V. I. (2011). Exopolysaccharides produced by bacteria isolated from the pelagic Southern Ocean—Role in Fe binding, chemical reactivity, and bioavailability. *Marine Chemistry*, 123(1–4), 88–98.
- Hassler, C. S., Norman, L., Mancuso Nichols, C. A., Clementson, L. A., Robinson, C., Schoemann, V., et al. (2015). Iron associated with exopolymeric substances is highly bioavailable to oceanic phytoplankton. *Marine Chemistry*, 173, 136–147. <https://doi.org/10.1016/j.marchem.2014.10.002>
- Hassler, C. S., Schoemann, V., Nichols, C. M., Butler, E. C. V., & Boyd, P. W. (2011). Saccharides enhance iron bioavailability to Southern Ocean phytoplankton. *Proceedings of the National Academy of Sciences of the United States of America*, 108(3), 1076–1081. <https://doi.org/10.1073/pnas.1010963108>
- Hatcher, P. G., Maciel, G. E., & Dennis, L. W. (1981). Aliphatic structure of humic acids: A clue to their origin. *Organic Geochemistry*, 3(1), 43–48.
- Hertkorn, N., Benner, R., Frommberger, M., Schmitt-Kopplin, P., Witt, M., Kaiser, K., et al. (2006). Characterization of a major refractory component of marine dissolved organic matter. *Geochimica et Cosmochimica Acta*, 70(12), 2990–3010. <https://doi.org/10.1016/j.gca.2006.03.021>
- Hutchins, D. A., Witter, A. E., Butler, A., & Luther, G. W. (1999). Competition among marine phytoplankton for different chelated iron species. *Nature*, 400(6747), 858–861.
- Kinsey, J. D., Corradino, G., Ziervogel, K., Schnetzer, A., & Osburn, C. L. (2018). Formation of chromophoric dissolved organic matter by bacterial degradation of phytoplankton-derived aggregates. *Frontiers in Marine Science*, 4(430).
- Kitayama, S., Kuma, K., Manabe, E., Sugie, K., Takata, H., Isoda, Y., et al. (2009). Controls on iron distributions in the deep water column of the North Pacific Ocean: Iron (III) hydroxide solubility and marine humic-type dissolved organic matter. *Journal of Geophysical Research*, 114, C08019. <https://doi.org/10.1029/2008JC004754>
- Kothawala, D. N., von Wachenfeldt, E., Koehler, B., & Tranvik, L. J. (2012). Selective loss and preservation of lake water dissolved organic matter fluorescence during long-term dark incubations. *Science of the Total Environment*, 433, 238–246. <https://doi.org/10.1016/j.scitotenv.2012.06.029>
- Laglera, L. M., Battaglia, G., & van den Berg, C. M. G. (2007). Determination of humic substances in natural waters by cathodic stripping voltammetry of their complexes with iron. *Analytica Chimica Acta*, 599(1), 58–66. <https://doi.org/10.1016/j.aca.2007.07.059>
- Laglera, L. M., Battaglia, G., & van den Berg, C. M. G. (2011). Effect of humic substances on the iron speciation in natural waters by CLE/CSV. *Marine Chemistry*, 127(1–4), 134–143.
- Laglera, L. M., & van den Berg, C. M. G. (2009). Evidence for geochemical control of iron by humic substances in seawater. *Limnology and Oceanography*, 54(2), 610–619.
- Maldonado, M. T., & Price, N. M. (1999). Utilization of iron bound to strong organic ligands by plankton communities in the subarctic Pacific Ocean. *Deep-Sea Research Part II: Topical Studies in Oceanography*, 46(11–12), 2447–2473.
- Mawji, E., Gledhill, M., Milton, J. A., Tarran, G. A., Ussher, S., Thompson, A., et al. (2008). Hydroxamate siderophores: Occurrence and importance in the Atlantic Ocean. *Environmental Science & Technology*, 42(23), 8675–8680. <https://doi.org/10.1021/es801884r>
- Millero, F. J. (1998). Solubility of Fe (III) in seawater. *Earth and Planetary Science Letters*, 154(1–4), 323–329.
- Moore, C. M., Mills, M. M., Arrigo, K. R., Berman-Frank, I., Bopp, L., Boyd, P. W., et al. (2013). Processes and patterns of oceanic nutrient limitation. *Nature Geoscience*, 6(9), 701–710. <https://doi.org/10.1038/ngeo1765>
- Moreau, S., Penna, A. D., Llort, J., Patel, R., Langlais, C., Boyd, P. W., et al. (2017). Eddy-induced carbon transport across the Antarctic Circumpolar Current. *Global Biogeochemical Cycles*, 31(9), 1368–1386. <https://doi.org/10.1002/2017GB005669>
- Mykkestad, S. M. (1995). Release of extracellular products by phytoplankton with special emphasis on polysaccharides. *Science of the Total Environment*, 165(1), 155–164.
- Nakayama, Y., Fujita, S., Kuma, K., & Shimada, K. (2011). Iron and humic-type fluorescent dissolved organic matter in the Chukchi Sea and Canada Basin of the western Arctic Ocean. *Journal of Geophysical Research*, 116, C07031. <https://doi.org/10.1029/2010JC006779>
- Nelson, N. B., Siegel, D. A., Carlson, C. A., & Swan, C. M. (2010). Tracing global biogeochemical cycles and meridional overturning circulation using chromophoric dissolved organic matter. *Geophysical Research Letters*, 37, L03610. <https://doi.org/10.1029/2009GL042325>
- Reygondeau, G., Longhurst, A., Martinez, E., Beaugrand, G., Antoine, D., & Mauray, O. (2013). Dynamic biogeochemical provinces in the global ocean. *Global Biogeochemical Cycles*, 27, 1046–1058. <https://doi.org/10.1002/gbc.20089>
- Romera-Castillo, C., Sarmiento, H., Alvarez-Salgado, X. A., Gasol, J. M., & Marrase, C. (2011). Net production and consumption of fluorescent colored dissolved organic matter by natural bacterial assemblages growing on marine phytoplankton exudates. *Applied and Environmental Microbiology*, 77(21), 7490–7498. <https://doi.org/10.1128/AEM.00200-11>
- Rosenstock, B., Zwiler, W., & Simon, M. (2005). Bacterial consumption of humic and non-humic low and high molecular weight DOM and the effect of solar irradiation on the turnover of labile DOM in the Southern Ocean. *Microbial Ecology*, 50(1), 90–101.
- Rue, E. L., & Bruland, K. W. (1995). Complexation of iron (III) by natural organic-ligands in the Central North Pacific as determined by a new competitive ligand equilibration adsorptive cathodic stripping voltammetric method. *Marine Chemistry*, 50(1–4), 117–138.
- Sedwick, P. N., DiTullio, G. R., Hutchins, D. A., Boyd, P. W., Griffiths, F. B., Crossley, A. C., et al. (1999). Limitation of algal growth by iron deficiency in the Australian Subantarctic region. *Geophysical Research Letters*, 26(18), 2865–2868. <https://doi.org/10.1029/1998GL002284>
- Sheng, G.-P., Xu, J., Luo, H. W., Li, W. W., Li, W. H., Yu, H. Q., et al. (2013). Thermodynamic analysis on the binding of heavy metals onto extracellular polymeric substances (EPS) of activated sludge. *Water Research*, 47(2), 607–614. <https://doi.org/10.1016/j.watres.2012.10.037>
- Shimotori, K., Omori, Y., & Hama, T. (2009). Bacterial production of marine humic-like fluorescent dissolved organic matter and its biogeochemical importance. *Aquatic Microbial Ecology*, 58(1), 55–66.

- Slagter, H. A., Laglera, L. M., Sukekava, C., & Gerringa, L. J. A. (2019). Fe-binding organic ligands in the humic-rich TransPolar Drift in the surface Arctic Ocean using multiple voltammetric methods. *Journal of Geophysical Research: Oceans*, 124, 1491–1508. <https://doi.org/10.1029/2018JC014576>
- Slagter, H. A., Reader, H. E., Rijkenberg, M. J. A., van der Rutgers Loeff, M., de Baar, H. J. W., & Gerringa, L. J. A. (2017). Organic Fe speciation in the Eurasian Basins of the Arctic Ocean and its relation to terrestrial DOM. *Marine Chemistry*, 197, 11–25. <https://doi.org/10.1016/j.marchem.2017.10.005>
- Stolpe, B., & Hassellöv, M. (2010). Nanofibrils and other colloidal biopolymers binding trace elements in coastal seawater: Significance for variations in element size distributions. *Limnology and Oceanography*, 55(1), 187–202.
- Sukekava, C., Downes, J., Slagter, H. A., Gerringa, L. J. A., & Laglera, L. M. (2018). Determination of the contribution of humic substances to iron complexation in seawater by catalytic cathodic stripping voltammetry. *Talanta*, 189, 359–364. <https://doi.org/10.1016/j.talanta.2018.07.021>
- Tagliabue, A., Aumont, O., DeAeth, R., Dunne, J. P., Dutkiewicz, S., Galbraith, E., et al. (2016). How well do global ocean biogeochemistry models simulate dissolved iron distributions? *Global Biogeochemical Cycles*, 30, 149–174. <https://doi.org/10.1002/2015GB005289>
- Tagliabue, A., Sallée, J. B., Bowie, A. R., Lévy, M., Swart, S., & Boyd, P. W. (2014). Surface-water iron supplies in the Southern Ocean sustained by deep winter mixing. *Nature Geoscience*, 7(4), 314–320. <https://doi.org/10.1038/ngeo2101>
- Tan, K. H., & Clark, F. E. (1969). Polysaccharide constituents in fulvic and humic acids extracted from soil. *Geoderma*, 2(3), 245–255.
- Ternon, E., Guieu, C., Loÿe-Pilot, M. D., Leblond, N., Bosc, E., Gasser, B., et al. (2010). The impact of Saharan dust on the particulate export in the water column of the North Western Mediterranean Sea. *Biogeosciences*, 7(3), 809–826. <https://doi.org/10.5194/bg-7-809-2010>
- Thuróczy, C. E., Gerringa, L. J. A., Klunder, M. B., Middag, R., Laan, P., Timmermans, K. R., & de Baar, H. J. W. (2010). Speciation of Fe in the Eastern North Atlantic Ocean. *Deep Sea Research Part I: Oceanographic Research Papers*, 57(11), 1444–1453. <https://doi.org/10.1016/j.dsr.2010.08.004>
- Trull, T. W., Bray, S. G., Manganini, S. J., Honjo, S., & François, R. (2001). Moored sediment trap measurements of carbon export in the Subantarctic and Polar Frontal zones of the Southern Ocean, south of Australia. *Journal of Geophysical Research*, 106(C12), 31,489–31,509.
- van den Berg, C. M. G. (1995). Evidence for the organic complexation of iron in seawater. *Marine Chemistry*, 50(1–4), 139–157.
- Velasquez, I. B., Ibisami, E., Maas, E. W., Boyd, P. W., Nodder, S., & Sander, S. G. (2016). Ferrioxamine siderophores detected amongst iron binding ligands produced during the remineralization of marine particles. *Frontiers in Marine Science*, 3(172).
- Wagener, T., Guieu, C., & Leblond, N. (2010). Effects of dust deposition on iron cycle in the surface Mediterranean Sea: Results from a mesocosm seeding experiment. *NBiogeosciences*, 7(11), 3769–3781.
- Whitby, H., & van den Berg, C. M. G. (2015). Evidence for copper-binding humic substances in seawater. *Marine Chemistry*, 173, 282–290.
- Wu, J., & Luther, G. W. (1995). Complexation of Fe (III) by natural organic ligands in the Northwest Atlantic Ocean by a competitive ligand equilibration method and a kinetic approach. *Marine Chemistry*, 50(1), 159–177.
- Wuttig, K., Wagener, T., Bressac, M., Dammshäuser, A., Streu, P., Guieu, C., & Croot, P. (2013). Impacts of dust deposition on dissolved trace metal concentrations (Mn, Al and Fe) during a mesocosm experiment. *Biogeosciences*, 4, 2583–2600.
- Zigah, P. K., McNichol, A. P., Xu, L., Johnson, C., Santinelli, C., Karl, D. M., & Repeta, D. J. (2017). Allochthonous sources and dynamic cycling of ocean dissolved organic carbon revealed by carbon isotopes. *Geophysical Research Letters*, 44, 2407–2415. <https://doi.org/10.1002/2016GL071348>